Supporting Information

Fluorometric detection of a chemical warfare agent mimic (DCP) using a simple hydroxybenzthiazole-diaminomaleonitrile based chemodosimeter

Manas kumar Das,[a] Tanushree Mishra,[a] Subhajit Guria,[a] Debojyoti Das,[a] Juheli Sadhukhan,[a] Sushmita Sarker,[c] Koushik Dutta,[b] Arghya Adhikary,[c] Dipankar Chattopadhyay,[b] Susanta Sekhar Adhikari,[a] *

[a]Department of Chemistry, University of Calcutta, 92, A.P.C. Road, Kolkata 700 009, West Bengal, India.

[b]Centre for Research in Nanoscience& Nanotechnology, (CRNN), University of Calcutta, Technology Campus, Sector-III, Block-JD 2, Salt Lake, Kolkata 700098, West Bengal, India.

[c]Center for Research in Nanoscience and Nanotechnology, Technology Campus, University of Calcutta, JD-2, Sector-III, Salt Lake, Kolkata-700106, West Bengal, India

* To whom correspondence should be addressed.

E-mail address: adhikarisusanta@yahoo.com

1. General method of UV-Vis and fluorescence titration

Path length of the cells used for absorption and emission studies was 1 cm. For UV-Vis and fluorescence titrations, stock solutions of the ligands were prepared in acetonitrile solvent. An appropriate amount of the ligands were pipetted in the cuvette so that the final volume of the ligand is 20 µM in buffer solution. Fluorescence measurements were performed using 5 nm x 5 nm slit width.

2. Buffer solution preparation

Buffer solutions were prepared according to the literature procedure. All the buffer solutions that are used are shown below, and are freshly prepared prior to use. pH of the solutions was measured using a pH meter and adjusted with HCl or NaOH to the desired value.

pH 2	KCl-HCl Buffer
pH 4	K_2HPO_4-HCl Buffer
pH 6	KH_2PO_4-NaOH Buffer
pH 7.4	Na_2HPO_4- KH_2PO_4-NaCl Buffer
pH 8	KH_2PO_4-NaOH Buffer
pH 10	Glycine-NaOH Buffer
pH 12	Na_2HPO_4- KH_2PO_4Buffer

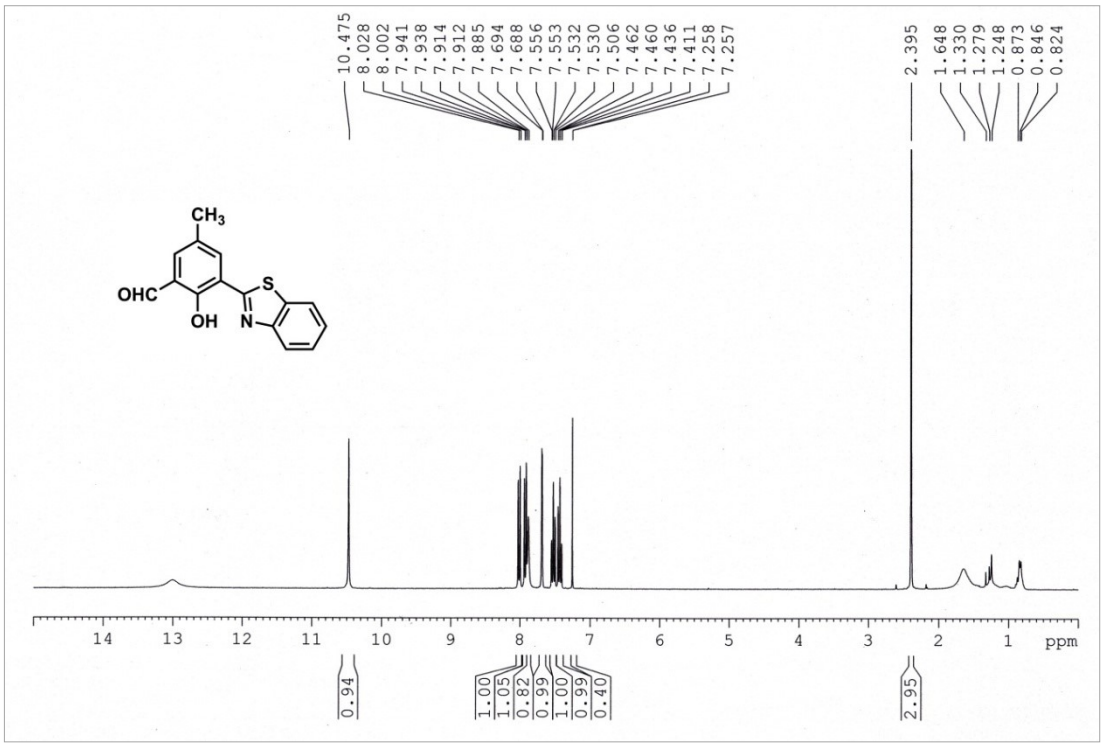

Figure S1: ^{1}H-NMR (300 MHz) of compound **BZ-CHO** in DMSO-d_6

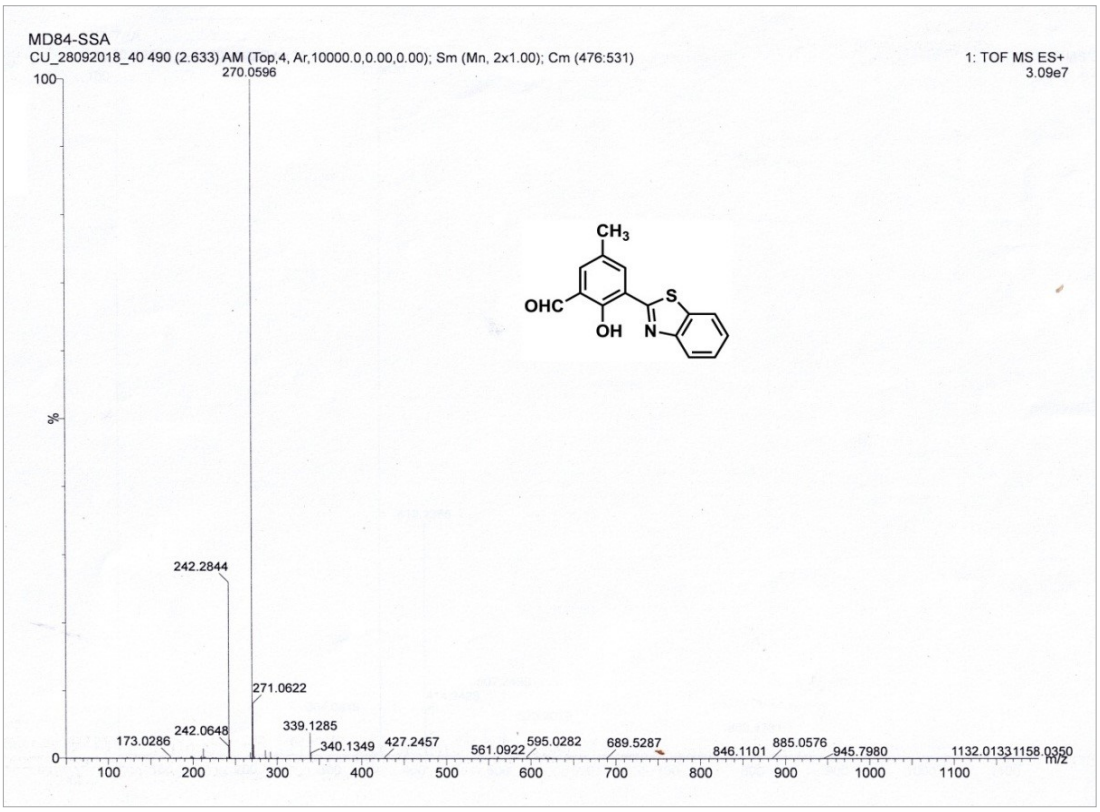

Figure S2: ESI-MS of compound **BZ-CHO**

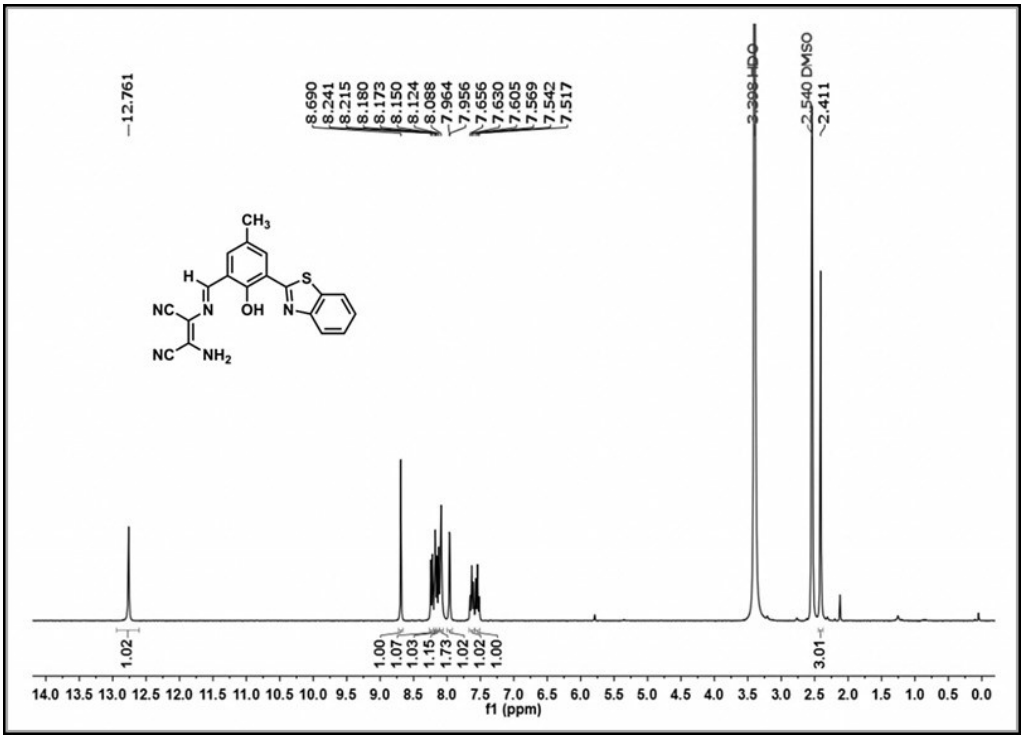

Figure S3: ^{1}H-NMR (500 MHz) of compound **BZ-DAM** in DMSO-d_6

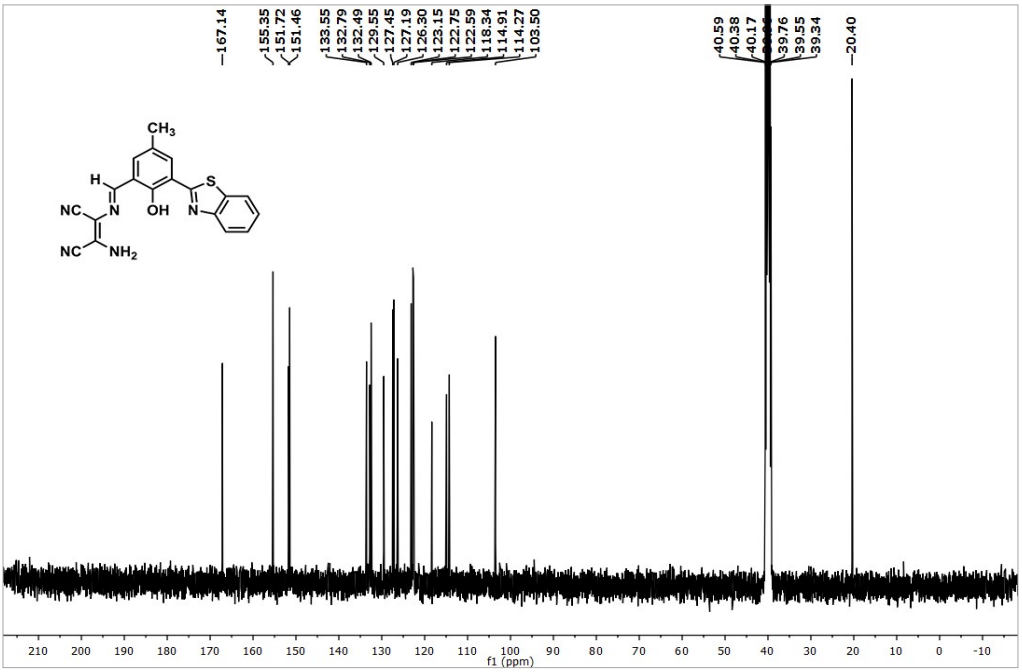

Figure S4: ^{13}C-NMR (100 MHz) of compound **BZ-DAM** in DMSO-d_6

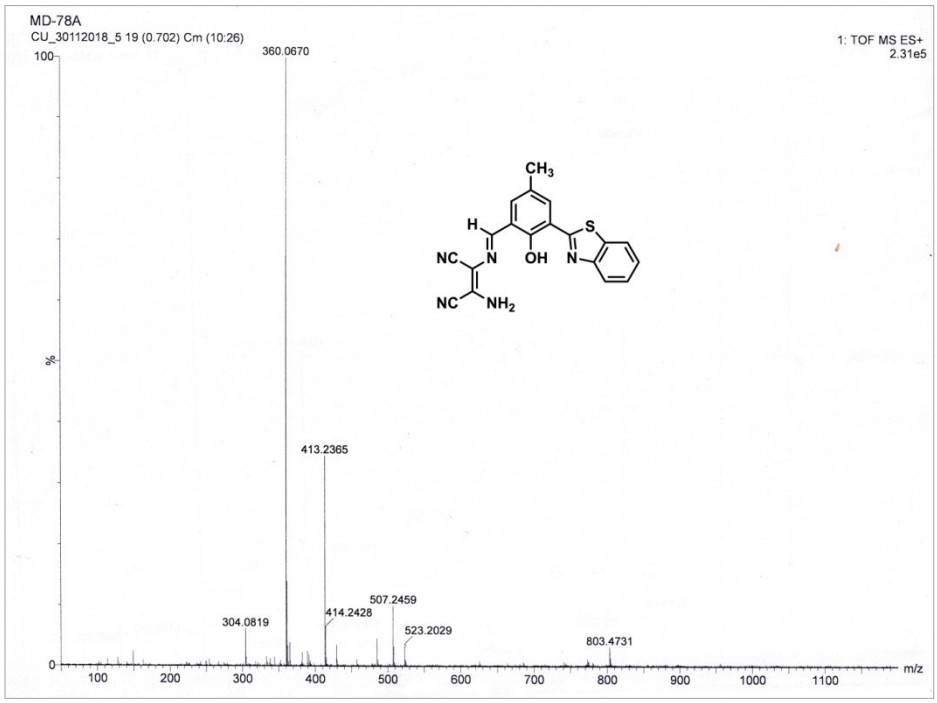

Figure S5: ESI-MS of compound **BZ-DAM**

Table S1: A comparison table for DCP probes

Structure of fluorescence probe	Nature of Fluorescence	Journal	Solvent system	Mechanism	LOD
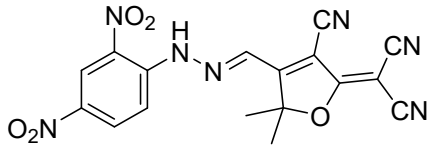	No fluorescence, only colour change	ACS Omega **2022**, 7, 5595–5604	CH_3CN	Deprotonation, Quinoid formation	25-200 ppm
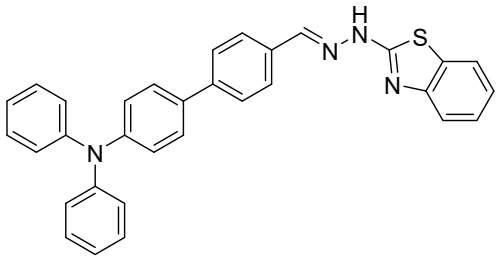	Fluorescence enhancement And ICT	OBC, **2022**, 20, 4803-4814	THF:H_2O (9:1)	Hydrolysis	35.6 nM
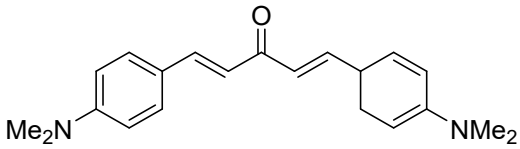	Fluorescence quenching	J. Mater. Chem. C, **2022**, 10, 5458–5465	CH_3CN-H_2O	Phosphamide formation	0.9 ppb

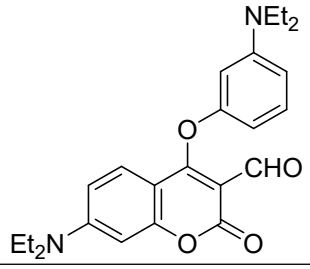	Fluorescence turns on and enhancement	ACS Appl. Bio. Mater. **2021**, 4, 7007-7015	DMSO	Cyclization	6.9 nM
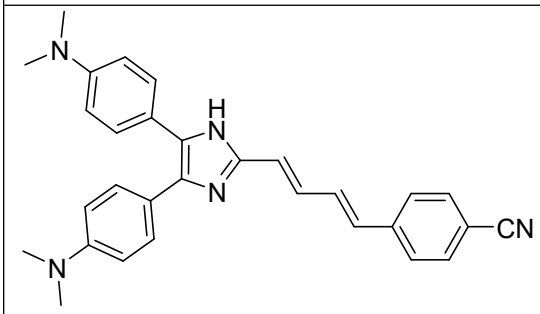	Fluorescence turns on and enhancement	J. Org. Chem. **2021**, 86, 14663−14671	H_2O	Phosphamide formation	35 ppb
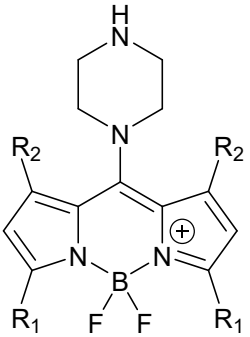	Fluorescence switches on and enhancement	Dyes and pigments, **2021**, 189, 109257	CH_3CN	Phosphamide formation, PET process	35 nM
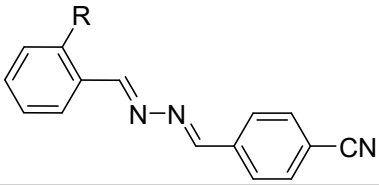	Fluorescence switches on and enhancement	Spectrochimica Acta Part A **2021**, 263, 120206	$CH_3CN:H_2O$(2:8)	Phosphorylation,	68 nM
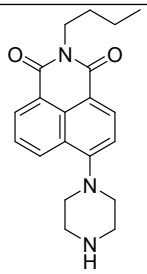	Enhancement of fluorescence	*New J. Chem.*, **2020,**44, 10713-10718	DMF	Phosphamide formation	5.5 nM
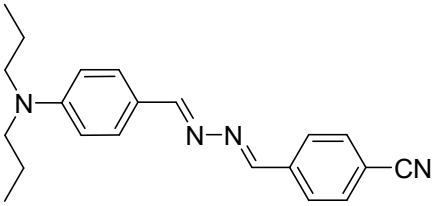	Fluorescence enhancement	RSC Adv., **2020**, 10, 25848–25855	THF:H_2O (3:7)	Phosphorylation, ICT	106 mM

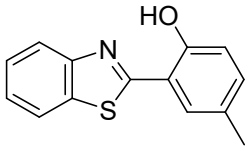	Fluorescence enhancement	Sensors & Actuators: B. Chemical **2020**, 319, 128282	CH_3CN	Phosphorylation, ESIPT	0.186 µM.
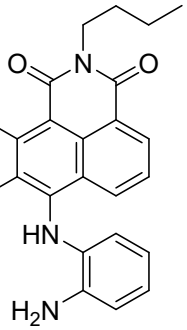	Fluorescence enhancement	Anal. Chem. **2019**, 91, 12070−12076	$CHCl_3$	Phosphamide formation	88 nM
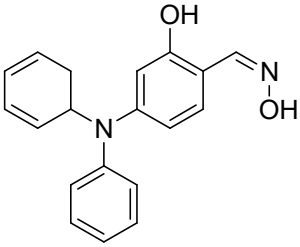	Fluorescence enhancement, Inhibition of PET	Dyes and Pigments **2019**, 170, 107585	CH_3CN-H_2O (4:6 v/v, 10mM HEPES buffer, pH 7.4)	Phosphamide formation	0.23 µM
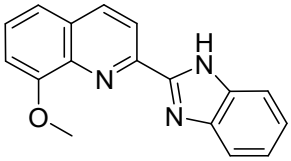	Ratiometric emission enhancement, ICT process	New J. Chem., **2019**, 43, 8627-8633	$CHCl_3$	Phosphamide formation, ICT	93.8 nM
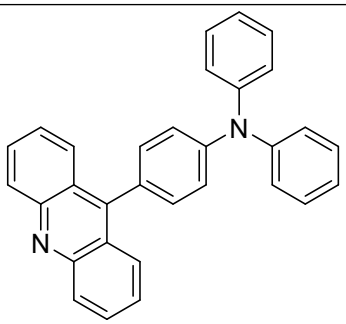	Quenching of fluorescence	Analytical Chemistry**2019**, 91, 17, 10927-10931	Water	Phosphamide formation,	0.15 ppb
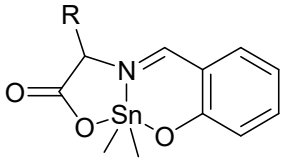	Quenching of fluorescence	New J. Chem.**, 2018,**42**,** 8756-8764	MeOH	Phosphorylation	6.88 µM
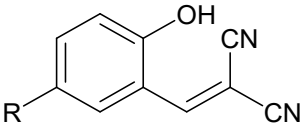	Fluorescence on and enhancement	Analyst**, 2018,**143**,** 4171-4179	CH_3CN-H_2O (10 mM HEPES buffer, 7:3 V/V, pH 7.4)	Phosphorylation	0.20 µM

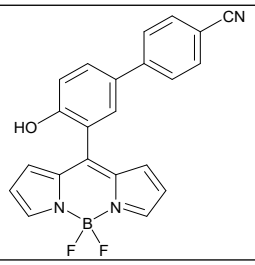	Fluorescence colour change and enhancement	Sensors and Actuators B **2018**, 255176–182	DMF	Phosphorylation	1.87 ppb
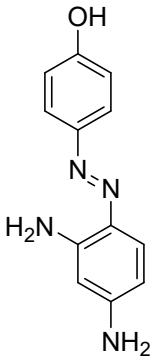	Quenching of fluorescence	Sensors and Actuators B **2017**, 242,977–982	CH_3CN	Phosphamide formation	0.2 mM.
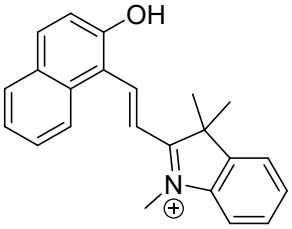	Dual emission intensities, emission Shift and enhancement	Org. Biomol. Chem., **2017**, 15, 5959–5967	$CH_3CN–H_2O$ (10.0 mM HEPES buffer, 1 : 1 v/v, pH 7.4)	Phosphorylation	18.86 nM
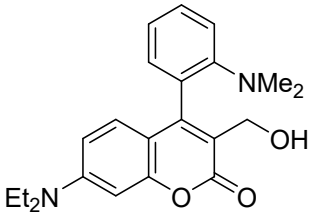	Enhancement in fluorescence intensity, PET process	*New J. Chem.***,** **2017,**41**,** 1653-1658	$CHCl_3$	Phosphorylation, cyclization	44 nM
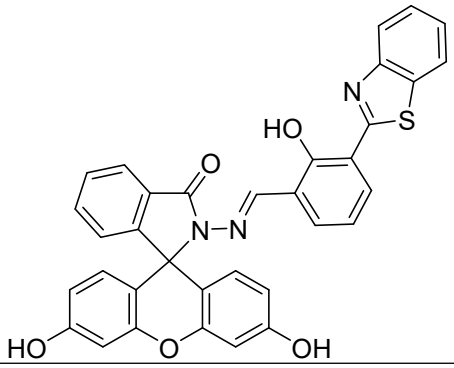	Fluorescence enhancement and blue shift	New J. Chem., **2017**,41, 6661-6666	DMSO (with 1% Et_3N	Phosphorylation,	1.6 µM

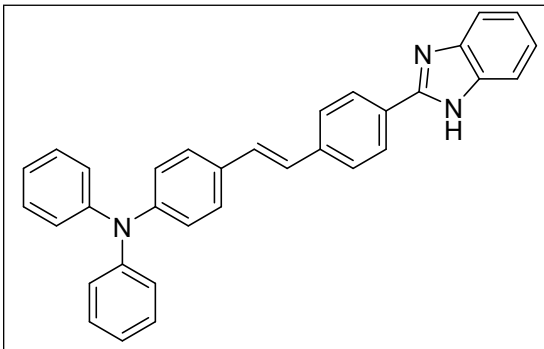	Fluorescence colour change and ICT enhancement	New J. Chem., **2017**,41, 12562-1256	THF/H_2O (4/1, v/v)	Phosphamide formation	84.5 nM
Present work 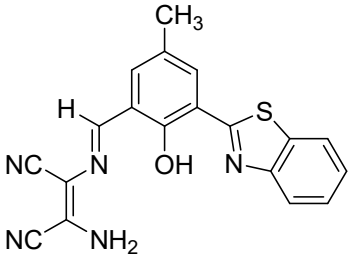	Fluorescence colour change via ESIPT process	--	CH_3CN–H_2O (1:1)	Phosphorylation followed by hydrolysis	0.43 µM

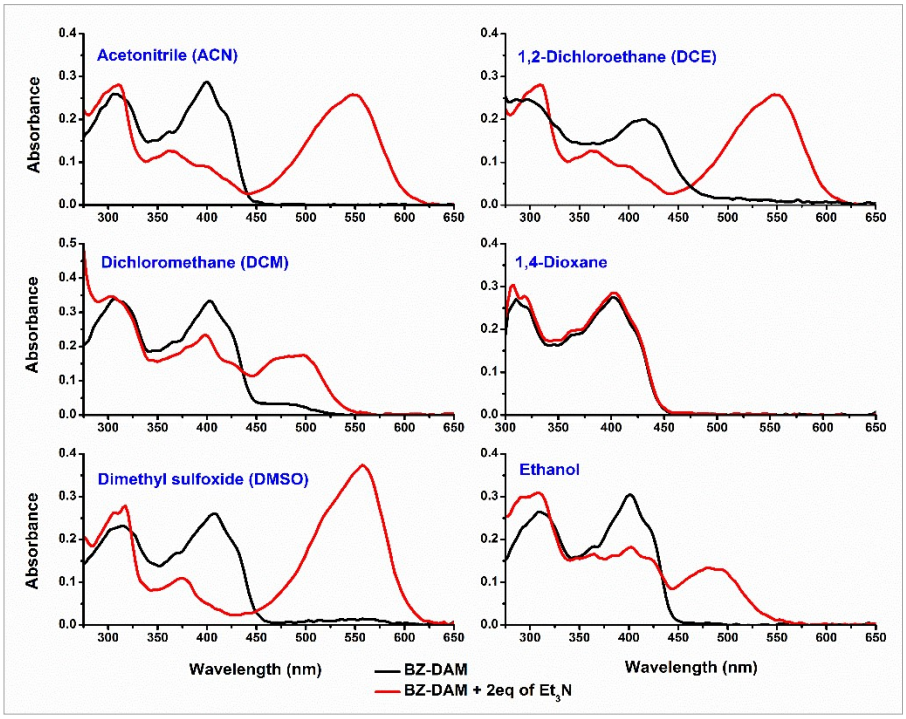

Figure S6. Absorption spectrum of BZ-DAM (20 µM) in solvents of varying polarity, in absence and in presence of 2eq of Triethylamine.

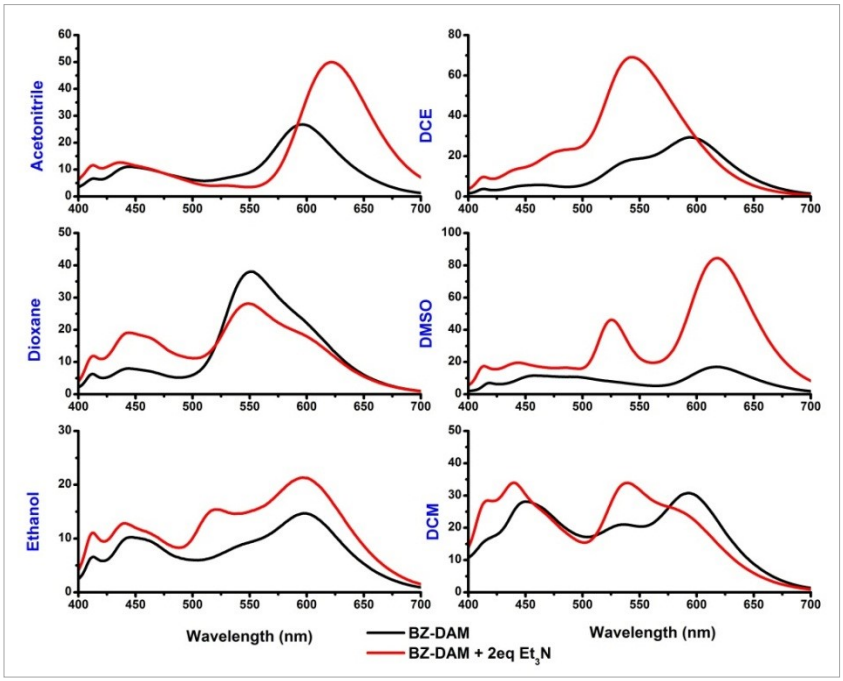

Figure S7. Normalized fluorescence spectrum of BZ-DAM (20 µM) in solvents of varying polarity, in absence and in presence of 2eq of Triethylamine.

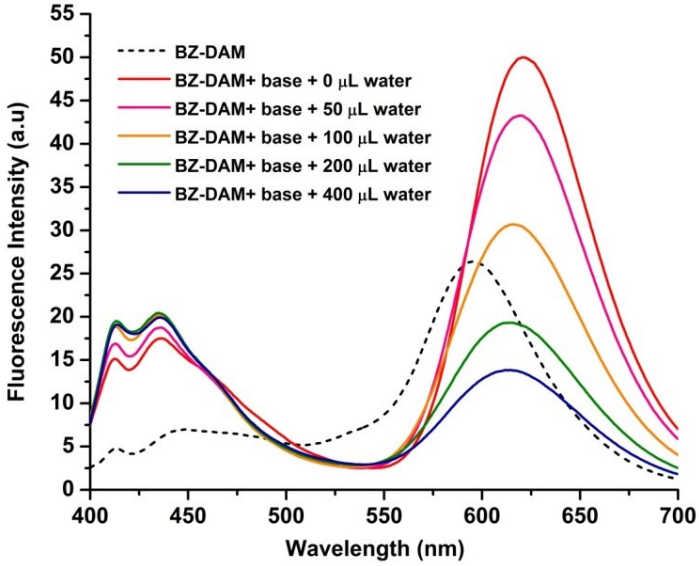

Figure S8: Fluorescence emission spectra of BZ-DAM (20 µM) in acetonitrile/water medium in presence of 4 eq. of Triehylamine.

Table S2: Summary of the lifetime of BZ-DAM in absence and in presence of DCP in (1:1) ACN:Water medium.

Species	τ_1 (ns)	B_1	τ_2 (ns)	B_2	τ_3 (ns)	B_3	χ^2	τ_{avg}
L @540	1.5	0.07	5.34	0.42	0.18	0.51	1.04	0.33
L @600	0.16	0.83	0.38	0.17	-	-	0.98	0.17
L @625	-	-	-	-	-	-	-	-
L+DCP @540	1.88	0.08	3.75	0.92	-	-	1.03	3.46
L+DCP @600	0.23	0.11	3.58	0.89	-	-	1.07	1.40
L+DCP @625	0.87	0.04	3.67	0.78	0.18	0.17	1.12	0.83

Table S3: Shift of proton in ^{1}H NMR titration of BZ-DAM in presence of DCP in DMSO-d_6

Proton	**Lig**	**0.5eq**	**1eq**	**1.5eq**	**2eq**
a	12.73	-	-	-	-
b	-	10.34	10.30	10.29	10.27
c	**8.66**	**8.65**	**8.62**	**8.63**	**8.59**
d	8.2-8.18	8.21-8.18	8.17-.15	8.17-8.14	8.15-8.12
e	**8.15-8.14**	**8.15**	**8.12-8.11**	**8.12-8.11**	**8.08**
f	8.12-8.09	8.11-8.09	8.08-8.06	8.09-8.06	8.06-8.04
g	8.06	-	-	-	-
h	**7.93-7.92**	**7.92-7.93**	**7.88-7.87**	**7.89**	**7.84**
i	7.62-7.57	7.62-7.57	7.60-7.55	7.61-7.56	7.59-7.54
J	7.54-7.49	7.53-7.48	7.52-7.46	7.52-7.47	7.51-7.45
k	-	-	7.70-7.69	7.72	7.69-7.68
l	**2.38**	**2.38**	**2.35**	**2.35**	**2.33**

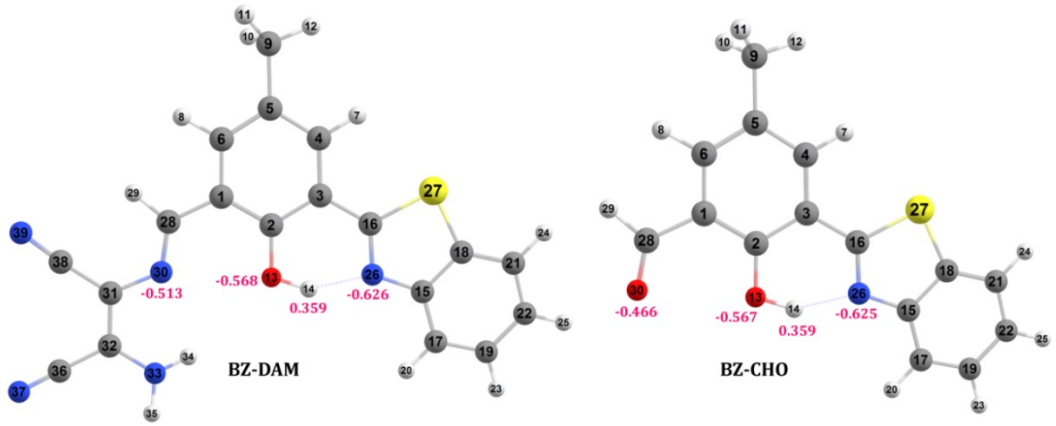

Figure S9: Geometry optimised structure of (a) BZ-DAM and (b) BZ-CHOat B3LYP/6-31G(d,p) level of theory. Mulliken charge density of the atoms involved in ESIPT process is written over the respective atom.

Table S4: Summary of the TDDFT electron transitions of keto and enol form of BZ-DAM and BZ-CHO at B3LYP/6-31G (d,p) level of theory.

Compound		Transitions corresponding to First excited state	ΔE (eV) between the orbitals	Normalized Coefficient (x)	Wavelength (nm) From TDDFT calculations	f_{osc}	Experimental wavelength (nm)
BZ-DAM	Enol-GS	HOMO-1→LUMO HOMO→LUMO HOMO→LUMO+1	3.71 3.37 3.94	0.29475 0.61922 -0.15494	414.57 nm	0.4825	400
	Enol-EX	HOMO-1→LUMO HOMO→LUMO HOMO→LUMO+1	3.50 2.86 3.54	-0.15323 0.67710 -0.11966	497.63 nm	0.8678	450
	Keto-EX	**HOMO→LUMO**	**2.49**	**-0.69999**	**613.02 nm**	**0.7528**	**595**
	Keto-GS	HOMO→LUMO	2.94	0.69588	494.08 nm	0.6041	------
BZ-CHO	Enol-GS	HOMO→LUMO	4.00	0.69195	358.36 nm	0.4401	366
	Enol-EX	HOMO→LUMO	3.56	0.70048	415.83 nm	0.7354	458
	Keto-EX	**HOMO→LUMO**	**2.96**	**0.70509**	**512.95 nm**	**0.5819**	**540**
	Keto-GS	HOMO→LUMO	3.33	0.70378	430.25 nm	0.4854	------

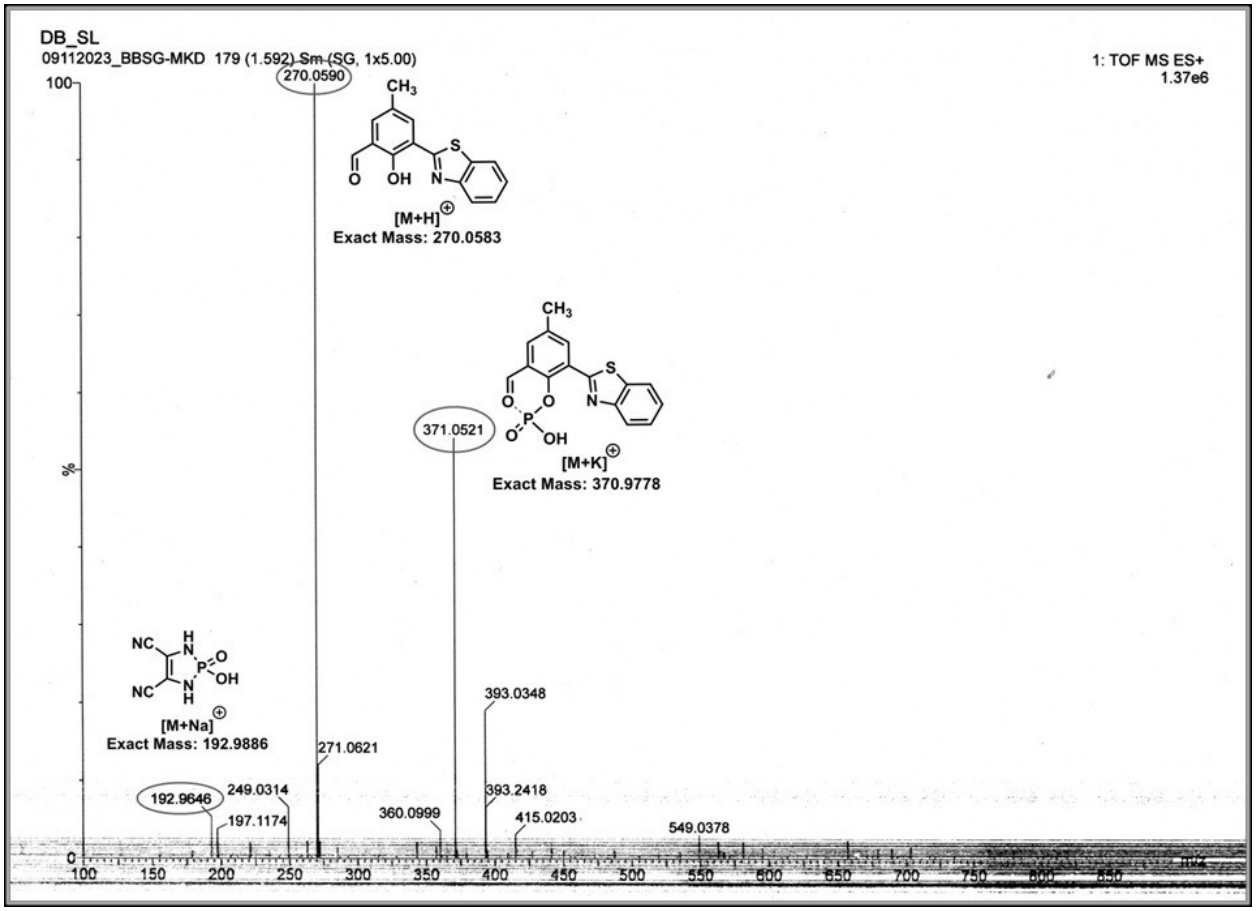

Figure S10: ESI-MS of compound **BZ-DAM** in presence of DCP

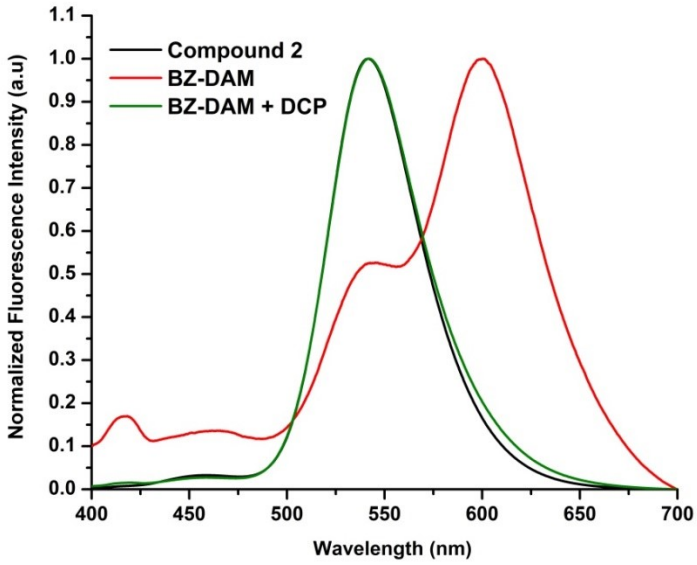

Figure S11: Comparison of Fluorescence emission spectra between Compound of BZ-CHO and BZ-DAM (20 µM) in (1:1) acetonitrile/water medium

Table S5: MTT assay data

Conc (ug/ml)	0	10	20	30	40	50	60	70	80	90	100
Abs 1	1.1878	0.6844	0.5056	0.6876	0.5616	0.586	0.3354	0.2536	0.344	0.4894	0.3284
Abs 2	0.8768	0.6718	0.5754	0.4832	0.4472	0.3724	0.485	0.2944	0.4628	0.4266	0.4308
Abs 3	0.4854	0.9302	0.5494	0.5974	0.4946	0.3928	0.3654	0.4762	0.4336	0.4162	0.341
Mean	**0.85**	**0.76213**	**0.54347**	**0.5894**	**0.50113**	**0.4504**	**0.39527**	**0.3414**	**0.41347**	**0.44407**	**0.36673**
SD	**0.35197**	**0.14569**	**0.03528**	**0.10243**	**0.05748**	**0.11788**	**0.07915**	**0.11851**	**0.06191**	**0.0396**	**0.05584**

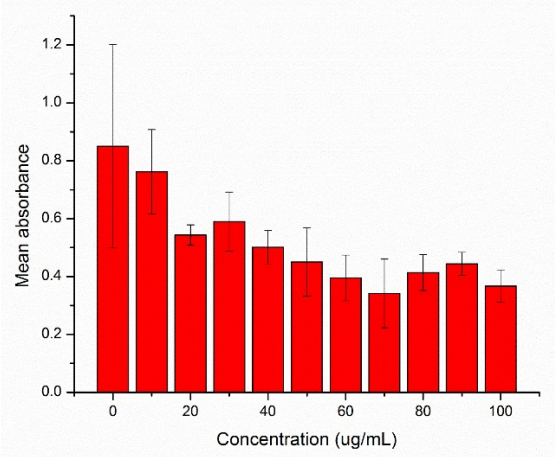

Figure S12: MTT assay bar diagram.

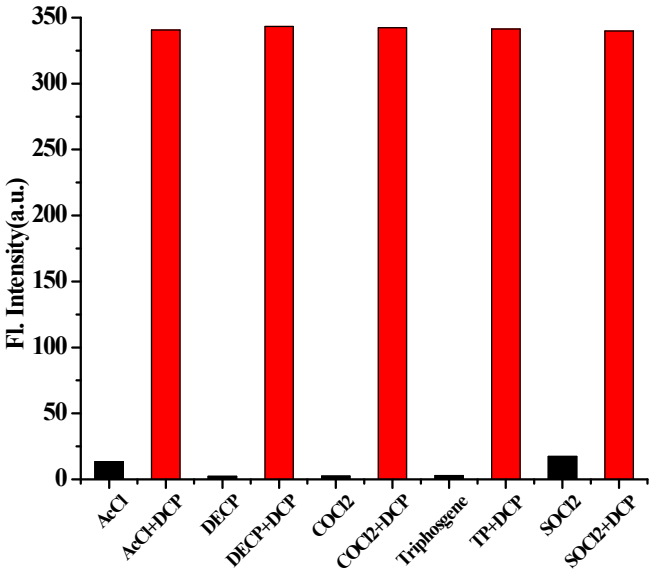

Figure S13: Change of emission intensity of BZ-DAM with DCP in presence of various analytes at 540 nm, in CH_3CN-H_2O (1:1) solution (λ_{ex} = 365 nm) at 25 °C.

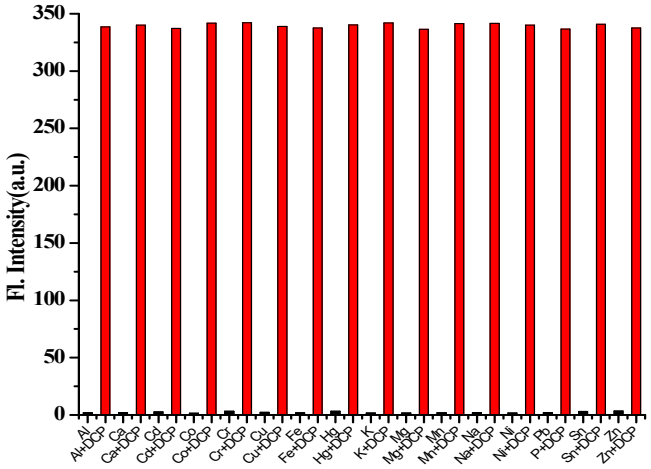

Figure S14: Change of emission intensity of BZ-DAM with DCP in presence of cations at 540 nm, in CH_3CN-H_2O (1:1) solution (λ_{ex} = 365 nm) at 25 °C.

In this mechanistic path, the phenol group in BZ-DAM is first phosphoesterified by DCP, which assists the formation of a significant 6-membered cyclic intermediate by the nucleophilic attack of a water molecule at the aldimine carbon atom and then followed by stepwise dephosphorylation to assist the complete hydrolysis of aldimine of BZ-DAM. The mechanism is supported by the mass spectra of the compound in presence of DCP.

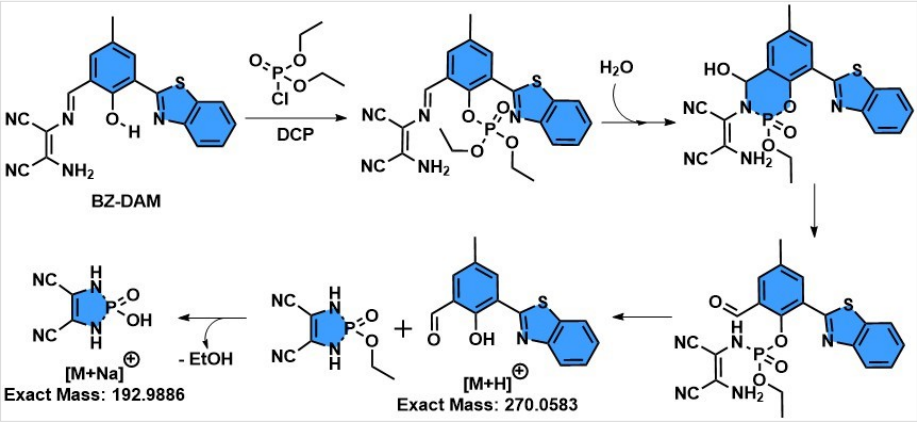

Figure S15: Plausible mechanism of hydrolysis of BZ-DAM (Aldemine) in presence of DCP in CH_3CN-H_2O (1:1) solution at 25 °C.

Here, initially both the ESIPT and ICT mechanisms are operative in the BZ-DAM. Thus, we can see two fluorescence bands: one at ~540 nm at another at ~600 nm. The red-shifted band (~ 600 nm) can be ascribed to the ESIPT-assisted ICT which can facilitate the delocalization of electrons on the DAM group.

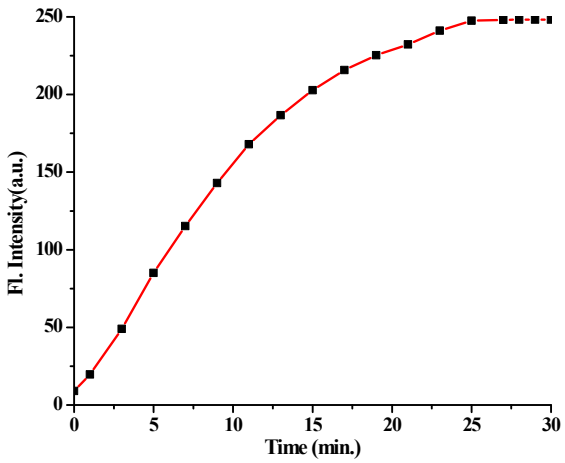

Figure S16: Changes in fluorescence intensity BZ-DAM with time in presence of DCP.

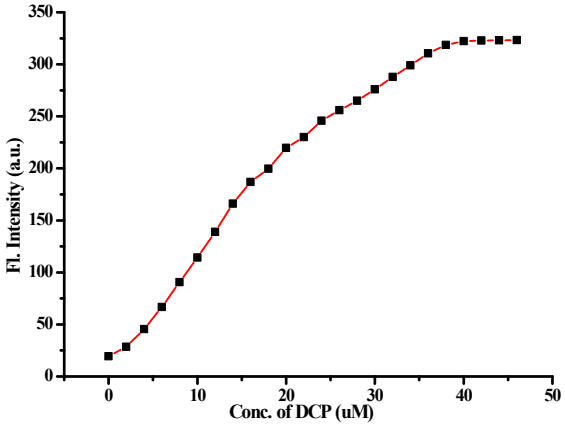

Figure S17: Changes in fluorescence intensity BZ-DAM of in presence of DCP at different concentration.

Determination of Detection Limit:

The detection limit (DL) of BZ-DAMfor DCP was determined from the following equation[1]:

DL = K* Sb1/S

Where K = 2 or 3 (we take 3 in this case); Sb1 is the standard deviation of the blank solution; S is the slope of the calibration curve.

From the graph we get slope = 7.3991, and Sb1 value is 1.068699.

Thus, using the formula, we get the Detection Limit = 0.433 µM i.e., BZ-DAM can detect DCP in this minimum concentration.

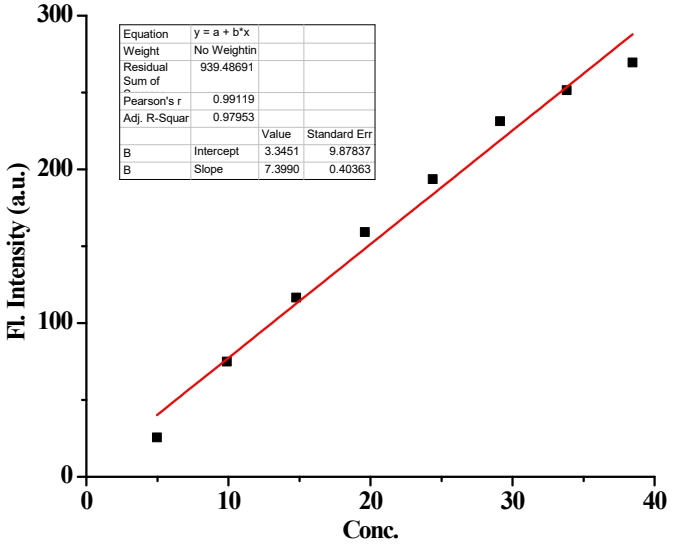

Figure S18: Linear fit plot ofLOD calculation of BZ-DAM with DCP.

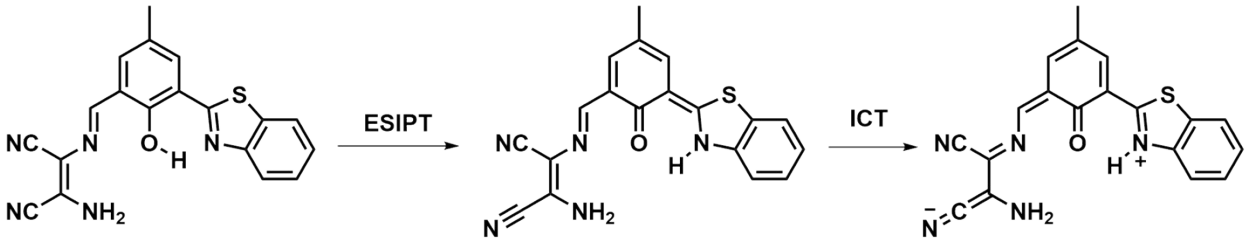

Figure S19: Mechanistic path of ESIPT assisted ICT process.

References:

1. Zhu, M.; Yuan, M.; Liu, X.; Xu, J.; Lv, J.; Huang, C.; Liu, H.; Li, Y.; Wang, S.; Zhu, D. *Org.Lett.* **2008,** *10,* 1481-1484.